JBIC (2000) 5 : 313–327

ORIGINAL ARTICLE

Ish K. Dhawan · Roopali Roy · Brian P. Koehler
Swaranalatha Mukund · Michael W.W. Adams
Michael K. Johnson

Spectroscopic studies of the tungsten-containing formaldehyde ferredoxin oxidoreductase from the hyperthermophilic archaeon *Thermococcus litoralis*

Received: 9 September 1999 / Accepted: 17 February 2000

Abstract The electronic and redox properties of the iron-sulfur cluster and tungsten center in the as-isolated and sulfide-activated forms of formaldehyde ferredoxin oxidoreductase (FOR) from *Thermococcus litoralis* (Tl) have been investigated by using the combination of EPR and variable-temperature magnetic circular dichroism (VTMCD) spectroscopies. The results reveal a $[Fe_4S_4]^{2+,+}$ cluster ($E_m = -368$ mV) that undergoes redox cycling between an oxidized form with an $S = 0$ ground state and a reduced form that exists as a pH- and medium-dependent mixture of $S = 3/2$ ($g = 5.4$; $E/D = 0.33$) and $S = 1/2$ ($g = 2.03$, 1.93, 1.86) ground states, with the former dominating in the presence of 50 % (v/v) glycerol. Three distinct types of W(V) EPR signals have been observed during dye-mediated redox titration of as-isolated Tl FOR. The initial resonance observed upon oxidation, termed the "low-potential" W(V) species ($g = 1.977$, 1.898, 1.843), corresponds to approximately 25–30 % of the total W and undergoes redox cycling between W(IV)/W(V) and W(V)/W(VI) states at physiologically relevant potentials ($E_m = -335$ and -280 mV, respectively). At higher potentials a minor "mid-potential" W(V) species, $g = 1.983$, 1.956, 1.932, accounting for less than 5 % of the total W, appears with a midpoint potential of -34 mV and persists up to at least +300 mV. At potentials above 0 mV, a major "high-potential" W(V) signal, $g = 1.981$, 1.956, 1.883, accounting for 30–40 % of the total W, appears at a midpoint potential of +184 mV. As-isolated samples of Tl FOR were found to undergo an approximately 8-fold enhancement in activity on incubation with excess Na_2S under reducing conditions and the sulfide-activated Tl FOR was partially inactivated by cyanide. The spectroscopic and redox properties of the sulfide-activated Tl FOR are quite distinct from those of the as-isolated enzyme, with loss of the low-potential species and changes in both the mid-potential W(V) species ($g = 1.981$, 1.950, 1.931; $E_m = -265$ mV) and high-potential W(V) species ($g = 1.981$, 1.952, 1.895; $E_m = +65$ mV). Taken together, the W(V) species in sulfide-activated samples of Tl FOR maximally account for only 15 % of the total W. Both types of high-potential W(V) species were lost upon incubation with cyanide and the sulfide-activated high-potential species is converted into the as-isolated high-potential species upon exposure to air. Structural models are proposed for each of the observed W(V) species and both types of mid-potential and high-potential species are proposed to be artifacts of ligand-based oxidation of W(VI) species. A W(VI) species with terminal sulfido or thiol ligands is proposed to be responsible for the catalytic activity in sulfide-activated samples of Tl FOR.

Key words Tungsten · Aldehyde ferredoxin oxidoreductase · Electron paramagnetic resonance · Magnetic circular dichroism · Iron-sulfur cluster

Abbreviations *AOR*: aldehyde ferredoxin oxidoreductase · *DMSOR*: dimethyl sulfoxide reductase · *EXAFS*: extended X-ray absorption fine structure · *FOR*: formaldehyde ferredoxin oxidoreductase · *GAPOR*: glyceraldehyde-3-phosphate ferredoxin oxidoreductase · *Pf*: *Pyrococcus furiosus* · *SO*: sulfite oxidase · *Tl*: *Thermococcus litoralis* · *VTMCD*: variable-temperature magnetic circular dichroism · *XO*: xanthine oxidase

Supplementary material. Figures S1 (MCD spectrum) and S2–S4 (EPR spectra) are available in electronic form on Springer-Verlag's server at http://link.springer.de/journals/jbic/

R. Roy · S. Mukund · M.W.W. Adams
Department of Biochemistry & Molecular Biology and Center for Metalloenzyme Studies, University of Georgia, Athens, GA 30602, USA

I.K. Dhawan · B.P. Koehler · M.K. Johnson (✉)
Department of Chemistry and Center for Metalloenzyme Studies, University of Georgia, Athens, GA 30602, USA
Tel.: +1-706-5429378
Fax: +1-706-5422353
e-mail: johnson@sunchem.chem.uga.edu

Introduction

Molybdenum- or tungsten-containing oxotransferases catalyze a wide variety of two-electron reactions involving net transfer of an oxygen atom between substrate and water [1–5]. In all cases the active site comprises a molybdenum or tungsten atom coordinated by the *cis*-enedithiolate functionality of a novel substituted pterin [6, 7]. The tricyclic ring structure of this substituted pterin cofactor (Fig. 1a) was first revealed in the X-ray crystal structure of the tungsten-containing aldehyde ferredoxin oxidoreductase from *Pyrococcus furiosus* (Pf) [8]. It has since been confirmed by the crystal structures of several pterin-cofactor-containing molybdoenzymes: chicken liver sulfite oxidase [9], aldehyde oxidoreductase from *Desulfovibrio gigas* [10, 11], dimethyl sulfoxide reductase from *Rhodobacter sphaeroides* [12] and *Rhodobacter capsulatus* [13–15], trimethylamine *N*-oxide from *Shewanella massilia* [16], dissimilatory nitrate reductase from *Desulfovibrio desulfuricans* [17], formate dehydrogenase H from *Escherichia coli* [18], and the tungsten-containing formaldehyde oxidoreductase from *Pyrococcus furiosus* [19].

On the basis of crystallographic, spectroscopic, primary sequence, mutagenesis, and cyanide inhibition studies, molybdenum/tungsten oxotransferases can be broadly classified into four subgroups that differ in terms of active site structure: sulfite oxidase (SO) family, xanthine oxidase (XO) family, dimethyl sulfoxide reductase (DMSOR) family, and aldehyde ferredoxin oxidoreductase (AOR) family (Fig. 1b) [4, 5]. Tungsten-containing enzymes are found in the DMSOR family and constitute the AOR family and in both cases the W center is coordinated by the dithiolates of two pterin cofactors. The nature of the sixth ligand in the AOR family has yet to be defined [oxo, sulfido, or an exogenous (non-protein) ligand cannot be ruled out at this stage], but it is clear that this family differs from the DMSOR family in having *no* protein ligation to the tungsten center.

Compared to the firmly established and essential role of molybdenum in global cycles, the role of tungsten in biological systems has just started to emerge [5, 20, 21]. During the past decade, at least a dozen tungstoenzymes have been purified [5]. Six distinct types of W-containing oxotransferases have been isolated, all of which contain one or more Fe-S clusters in addition to the W active site. AOR [22–24], formaldehyde ferredoxin oxidoreductase (FOR) [19, 25], and glyceraldehyde-3-phosphate ferredoxin oxidoreductase (GAPOR) [26] constitute the AOR family and all have been purified from hyperthermophilic archaea. The W-enzymes in the DMSOR family include formate dehydrogenase [27, 28] and carboxylic acid reductase from acetogenic bacteria [29, 30], and formylmethanofuran dehydrogenase from methanogenic archaea [31–33]. In general, these W-oxotransferases are found in thermophilic anaerobes and catalyze low-potential conversions (reduction potentials in the range −420 to −560 mV versus NHE) at the level of carboxylic acids and aldehydes.

Thermococcus litoralis (Tl) FOR is a tetrameric enzyme of 280 kDa molecular mass with each subunit containing one W center and one $[Fe_4S_4]$ cluster [25]. Chemical analysis has shown that Tl FOR contains the non-nucleotide form of the pterin cofactor [34] and, based on the high level of sequence homology [35] and analogous quaternary structure, it is closely related to the crystallographically defined Pf FOR [19]. The recent X-ray structure of Pf FOR at 1.85 Å resolution showed the enzyme to be a tetramer of 69 kDa subunits, each containing one W, one $[Fe_4S_4]$ cluster, and one Ca^{2+}. The structure and arrangement of the W and $[Fe_4S_4]$ centers are very similar to that of Pf AOR, but FOR lacks the monomeric Fe at its subunit interface. In addition to the four pterin-cofactor dithiolene sulfur ligands, the W center in each of the four subunits appears to be coordinated by a ter-

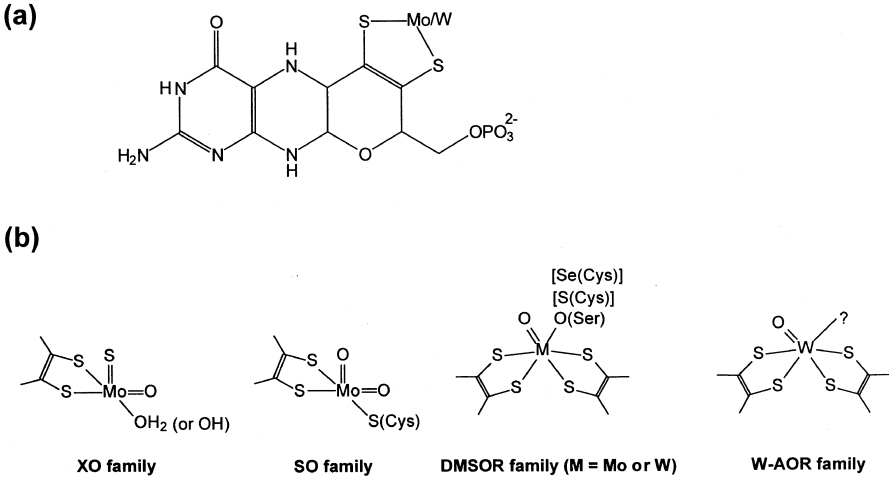

Fig. 1 **a** Crystallographically established structure of the pterin cofactor found in Mo/W oxotransferases and the mode of coordination to a Mo and W center. The terminal phosphate is elaborated as a guanine, adenine, or cytosine dinucleotide in some enzymes. **b** Proposed structures for the Mo(VI)/W(VI) forms of the four distinct families of Mo/W oxotransferases

minal oxo group. Although this group refines to a distance of 2.10 Å from W in Pf FOR, which would imply a W-OH or W-OH_2 linkage, this distance may be an artifact of electron density truncation effects [36] and could correspond to a W = O at about 1.7 Å. The catalytic properties of Tl FOR and Pf FOR are strikingly different from those of Pf AOR. While Pf AOR is capable of oxidizing a broad range of aliphatic and aromatic aldehydes, Tl FOR and Pf FOR oxidize only short C1-C3 chain length aldehydes. Furthermore, while it was discovered that reductive incubation with sodium sulfide and dithionite would restore activity to oxygen-inactivated Pf AOR, similar treatments of anaerobically purified samples of Tl FOR and Pf FOR resulted in a 5- to 8-fold increase in activity [37, 38].

Previously we have reported a detailed study on the electronic and redox properties of the Fe-S and W centers in the AOR from Pf and *Pyrococcus* strain ES-4 (ES-4) using the combination of electron paramagnetic resonance (EPR) and variable-temperature magnetic circular dichroism (VTMCD) spectroscopies [39]. The results revealed considerable heterogeneity at the W center in active preparations of both AORs and suggested that W(VI), W(V), and W(IV) species were all present in dithionite-reduced samples. The high-potential W(V) species (0.3 spins/W) was proposed to originate from an internal redox reaction involving a terminal S ligand (S^{2-} or -SH) and a W(VI) center. Such observations raised the possibility of the presence of a terminal sulfido or thiol group at the active site. Although W-XAS [40] and X-ray crystallography [8, 19] have shown no evidence for a terminal sulfido or thiol group, such a ligand might be difficult to detect if it were present in only 30 % of the sample. In the previous work we stressed a pressing need to obtain homogenous samples for spectroscopic investigations. Towards this end, we report here the spectroscopic, redox, sulfide activation, and cyanide inactivation properties of Tl FOR.

Materials and methods

Sample preparation

Samples of active FOR from Tl were purified and assayed as previously described [25]. All samples were purified anaerobically in 100 mM Tris/HCl buffer, pH 8.0, with 2 mM sodium dithionite, 2 mM dithiothreitol, and 10 % (v/v) glycerol. The as-isolated samples of Tl FOR used for spectroscopic studies exhibited specific activities in the range 6–10 units/mg, where 1 unit corresponds to 1 μM of formaldehyde oxidized/min at 80 °C. Sulfide activation experiments were performed as previously reported [37]. The as-isolated Tl FOR sample was incubated (8–10 mg/mL) with 100-fold excess of a buffered solution of sodium sulfide and dithionite for 8 h under anaerobic conditions to achieve optimal activation. The specific activity of the Tl FOR samples increased approximately 8-fold after sulfide activation. Excess sulfide was removed prior to cyanide-inactivation experiments. The sulfide-activated Tl FOR was loaded onto a column (1 × 18 cm) of Sephadex G-25 (Pharmacia LKB) previously equilibrated with 100 mM Tris/HCl buffer (pH 8.0) containing 2 mM dithionite and 2 mM DTT with a flow rate of 0.25 mL/min in order to remove excess sulfide and dithionite. The sample was eluted with the 100 mM Tris/HCl (pH 8.0) buffer and collected anaerobically. Fractions containing Tl FOR were concentrated to a final concentration of approximately 13 mg/mL by ultrafiltration. The specific activity of the resulting sulfide-activated form decreased by about 20 % following this procedure, but this specific activity remained unchanged even after a further 24 h under anaerobic conditions. Cyanide was added using a stock solution of potassium cyanide made up in 200 mM Tris/HCl buffer, pH 8.0.

The sample concentrations quoted in the figure legends are based on protein determinations using the Lowry method, with a correction factor applied based on direct amino acid analysis, and are expressed per monomer (M_r = 69,000). All samples were handled in a Vacuum Atmospheres glove box (< 1 ppm O_2) under an argon atmosphere. EPR redox titrations on as-isolated and sulfide-activated samples were performed at ambient temperature (25–27 °C) in the glove box under anaerobic conditions. Mediator dyes were added, each to a concentration of ca. 50 μM, in order to cover the desired range of redox potentials, i.e. methyl viologen, benzyl viologen, neutral red, safranin O, phenosafranin, anthraquinone-2-sulfonate, anthraquinone-1,5-disulfonate, 1,4-benzoquinone, indigo-disulfonate, 1,2-naphthoquinone, thionine, methylene blue, duroquinone, and 1,2-naphthoquinone-4-sulfonate. Samples were first reduced by addition of excess sodium dithionite followed by oxidative titration with potassium ferricyanide. After equilibration at the desired potential, a 0.2-mL aliquot was transferred to a calibrated EPR tube and immediately frozen in liquid nitrogen. Potentials were measured with a platinum working electrode and a saturated Ag/AgCl reference electrode. All redox potentials are reported relative to NHE.

Spectroscopic methods

Variable-temperature and variable-field MCD measurements were recorded on samples containing 50–55 % (v/v) glycerol using a Jasco J-500C (180–1000 nm) or J-730 (700–2000 nm) spectropolarimeter mated to an Oxford Instruments Spectromag 4000 (0–7 T) split-coil superconducting magnet. The experimental protocols for measuring MCD spectra of oxygen-sensitive samples over the temperature range 1.5–300 K with magnetic fields up to 7 T have been described elsewhere [41, 42]. X-band (~ 9.6 GHz) EPR spectra were recorded on a Bruker ESP-300E EPR spectrometer with a dual-mode ER-4116 cavity and equipped with an Oxford Instruments ESR-9 flow cryostat (4.2–300 K). Frequencies were measured with a Systron-Donner 6054B frequency counter and the field was calibrated with a Bruker ER 035M gaussmeter. Spin quantitations were carried out under non-saturating conditions using 1-mM CuEDTA as the standard. EPR spectral simulations were performed on IBM RISC 6000 computer in University Computing and Networking Services (UCNS) at the University of Georgia. Simulations of frozen solution EPR spectra were carried out using a modified version of the QPOW program developed by Prof. R. L. Belford and co-workers [43, 44]. The *g*- and *A*-tensors were taken to be collinear and Gaussian lineshapes were assumed for all simulations. The $I = 0$ and $I = 1/2$ components were simulated separately. Each simulated spectrum ($I = 0$ and $I = 1/2$ components) was quantified by double integration and contributions from the $I = 1/2$ (^{183}W isotope, 14.28 % natural abundance) and $I = 0$ (^{182,184,186}W isotopes, 85.72 % natural abundance) components were summed based on their natural abundances.

Results

Spectroscopic characterization of as-isolated Tl FOR

Dithionite-reduced Tl FOR

As for Pf and ES-4 AOR, initial studies of Tl FOR focused on the enzyme as-purified anaerobically in pH 8.0 Tris/HCl buffer in the presence of 2 mM sodium dithionite. Perpendicular-mode EPR studies (Fig. 2, inset) reveal that dithionite-reduced Tl FOR contains paramagnetic centers with both $S = 3/2$ and $S = 1/2$ ground states, as evidenced by the broad resonance at $g = 5.4$ and the rhombic $g = 2.03$, 1.93, and 1.86 resonances, respectively. These signals arise from fast relaxing species and were not observable above 30 K. The absorption-shaped peak at $g = 5.4$ is attributed to a completely rhombic $S = 3/2$ ground state ($E/D = 0.33$) with zero-field splitting greater than the Zeeman splitting, which leads to effective g values of 5.4, 2.0, and 1.4 for both doublets. The features at $g = 2.0$ and 1.4 are expected to be broad and difficult to observe, and are additionally obscured by the rhombic $S = 1/2$ resonance ($g = 2.03$, 1.93, 1.86) which accounts for 0.2 spins/molecule at pH 8.0. The intensity ratio of these two resonances is dependent on the pH and sample medium. Increasing the pH to 10 results in a 2- to 4-fold increase in the $S = 1/2$ component, whereas the addition of 50 % glycerol decreases the $S = 1/2$ component by a factor of approximately 2. Mixed-spin $[Fe_4S_4]^+$ clusters with medium-dependent $S = 1/2$ and $S = 3/2$ ground state mixtures have been previously observed in other biological systems [45, 46]. Hence, the $[Fe_4S_4]^+$ cluster in Tl FOR is predominately $S = 3/2$ at pH 8 in the absence of glycerol and almost exclusively $S = 3/2$ in the presence of 50 % glycerol.

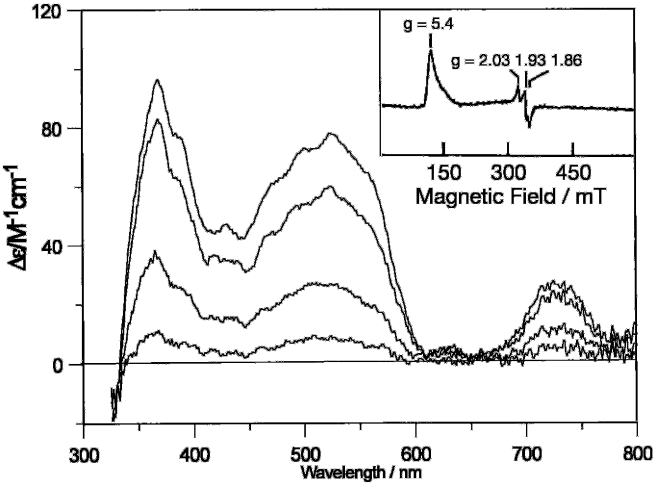

Fig. 2 VTMCD spectra of dithionite-reduced Tl FOR. The final solution was 0.21 mM in FOR with 55 % (v/v) glycerol. Spectra recorded at temperatures of 1.89, 4.22, 10.3, and 24.5 K. The MCD spectra were recorded with an applied magnetic field of 4.5 T and the intensity of all transitions increases with decreasing temperature. *Inset*: X-band EPR spectrum of dithionite-reduced Tl FOR. The sample was 0.15 mM in FOR. EPR conditions: temperature, 4.2 K; microwave power, 1 mW; modulation amplitude, 0.63 mT, microwave frequency, 9.60 GHz

VTMCD spectroscopy has been well established as a means of investigating the ground and excited state properties of paramagnetic Fe-S clusters and provides a useful "fingerprint" for identifying the cluster type of paramagnetic Fe-S centers [45, 47–49]. The VTMCD spectra of dithionite-reduced Tl FOR containing 55 % (v/v) glycerol are shown in Fig. 2 and display temperature-dependent bands which closely resemble those observed for other $S = 3/2$ $[Fe_4S_4]^+$ clusters in general [45] and for the more axial $S = 3/2$ $[Fe_4S_4]^+$ cluster in Pf and ES-4 AORs in particular [39]. The predominant $S = 3/2$ ground state of the $[Fe_4S_4]^+$ cluster in Tl FOR is confirmed by VTMCD magnetization studies at 545 nm (see Fig. S1 in the Supplementary material). To a good approximation, the lowest temperature data are fit to a doublet with $g_{\|} = 5.4$ and $g_{\perp} = 1.8$, i.e. the effective g-values of the zero field doublets of a rhombic $S = 3/2$ system. In accordance with the EPR data, the fit is further improved by inclusion of a minor (10 %) contribution from a $S = 1/2$ species ($g = 2.03$, 1.93, 1.86).

Redox titration of Tl FOR

The redox properties of the $S = 3/2$ $[Fe_4S_4]^+$ cluster were monitored at 4 K by EPR spectroscopy via a dye-mediated oxidative redox titration (see Fig. S2 in Supplementary material). The signal intensity of the $S = 3/2$ $[Fe_4S_4]^+$ cluster versus sample redox potential fits well to a simple one-electron Nernst plot (solid line) and indicates a midpoint potential of -368 ± 20 mV for the $[Fe_4S_4]^{2+/+}$ couple (Fig. 3).

Previous EPR studies of Tl FOR did not report any resonances attributable to magnetically isolated W(V) species [25]. However, three distinct types of W(V) EPR signals with properties similar to those of the low-potential, mid-potential, and high-potential W(V) species found in Pf and ES-4 AOR were observed in dye-mediated redox titrations of Tl FOR. These resonances are shown in Fig. 4 and are attributed to magnetically isolated W(V) species based on the principal g-values ($g_{1,2,3} < 2$), the observation of resolved ^{183}W satellites ($I = 1/2$, 14.28 % natural abundance) in the more intense low-potential and high-potential species, and relaxation properties. The spectra shown in Fig. 4 were recorded at 40 K, but these resonances are all observable up to at least 100 K without any significant change in linewidth. The EPR parameters and midpoint potentials of these species are summarized and compared with those previously reported for Pf AOR in Table 1. No resonance corresponding to the glycerol-inhibited W(V) species seen in Pf and ES-4 AOR was observed or generated,

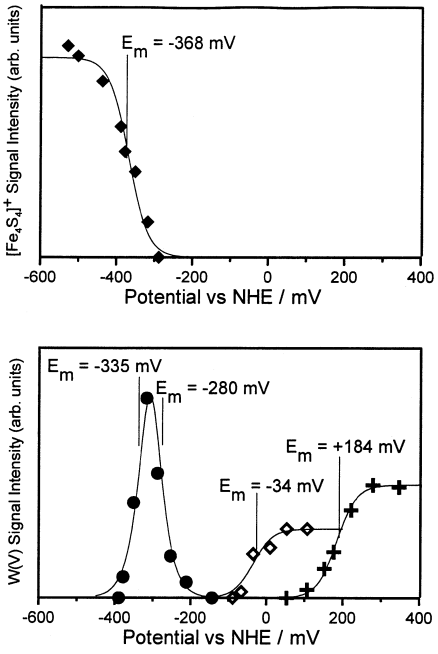

Fig. 3 EPR signal intensities (arbitrary units) for Tl FOR as a function of poised potential. Dye-mediated redox titrations were carried out as described in Materials and methods with active Tl FOR (0.11 mM) purified in the presence of 10 % (v/v) glycerol. *Upper panel*: intensity of the $g = 5.4$ component of $S = 3/2$ [4Fe-4S]$^{+}$ cluster (◆) at 4.2 K. *Lower panel*: peak-to-trough intensity of the $g = 1.898$ feature of the low-potential W(V) species (●), intensity of the $g = 1.932$ component of the mid-potential W(V) species (◇), and intensity of the $g = 1.883$ component of the high-potential W(V) species (+). All samples in the lower panel were measured at 40 K. *Solid lines* are best fits to one-electron Nernst equations or a two-electron Nernst equation for sequential one-electron oxidations with only the one-electron oxidized form EPR active. The midpoint potentials used in constructing the Nernst plots are indicated on the figure. EPR conditions: temperatures, as indicated; microwave power, 5 mW (upper panel) and 1 mW (lower panel); modulation amplitude, 0.643 mT; microwave frequency, 9.60 GHz

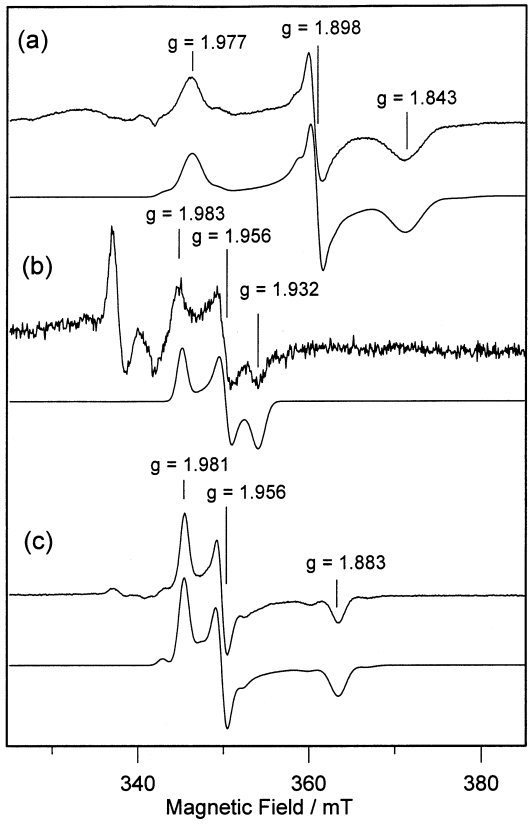

Fig. 4 X-band EPR spectra and simulations of the low-potential (**a**), mid-potential (**b**), and high-potential (**c**) W(V) species in Tl FOR. The low-potential sample was prepared by reduction with dithionite at pH 6.0, as described in the text. The mid-potential and high-potential samples were poised at +10 mV and +225 mV, respectively, by ferricyanide oxidation in the presence of redox dyes. The simulation parameters were: **a** $g_{1,2,3} = 1.977$, 1.898, 1.843; $A_{1,2,3} = 57$, 28, 50×10^{-4} cm^{-1}; $l_{1,2,3} = 1.37$, 0.67, 2.01 mT; **b** $g_{1,2,3} = 1.983$, 1.956, 1.932; $l_{1,2,3} = 0.70$, 0.54, 0.81 mT; **c** $g_{1,2,3} = 1.981$, 1.956, 1.883; $A_{1,2,3} = 45$, 40, 59×10^{-4} cm^{-1}; $l_{1,2,3} = 0.65$, 0.59, 1.04 mT; where l is the linewidth. Owing to the low signal intensity and lack of resolved ^{183}W satellites for the mid-potential signal **b**, only the $I = 0$ component has been simulated in this case. EPR conditions: temperature, 40 K; microwave power, 5 mW; modulation amplitude, 0.643 mT; microwave frequency, 9.60 GHz

even in the presence of 55 % glycerol. This is consistent with the observations that Tl FOR, unlike Pf and ES-4 AOR, is not inhibited by glycerol.

The initial resonance observed upon oxidation of Tl FOR is termed the low-potential signal, $g = 1.977$, 1.898, and 1.843 (Fig. 4a). As the potential is increased, the low-potential signal gradually increases, maximizes, and then subsequently decreases (see Fig. S3 in Supplementary material). The intensity of this resonance versus sample potential is plotted in Fig. 3. This behavior is interpreted in terms of two sequential one-electron oxidations (solid line) with only the one-electron oxidized form being EPR-active, yielding midpoint potentials of -335 ± 20 mV for the W(IV/V) couple and -280 ± 20 mV for the W(V/VI) couple. In redox titrations the low-field component of the resonance is partially obscured by a radical signal from the redox dyes. However, the low-potential species can also be generated without the obscuring radical signal, by modulating the potential of the solution either by using a milder reductant such as formamidinesulfinic acid in Tris/HCl pH 8 buffer, or by lowering the pH of the solution with MES pH 6.0 buffer with 5- to 10-fold excess of sodium dithionite. In contrast to Pf and ES-4 AORs, the low-potential resonance was not generated by incubation of the enzyme with formaldehyde at 80 °C, possibly due to the higher potentials for the W(IV)/(V) and W(V)/(VI) couples in Tl FOR. The low-potential EPR spectrum was simulated (Fig. 4a) in order to obtain the anisotropic g and $A(^{183}\mathrm{W})$ parameters listed in Table 1. Spin quantitation of the simulated spectra indicated a maximum intensity corresponding to 0.15 ± 0.05 spins/W. Scaling the spin quantitation data on the basis of the Nernst fit (Fig. 3) indicates that the W-species responsible for the W(V) low-potential

Table 1 EPR *g*-values, *A*-values ($cm^{-1} \times 10^4$), and midpoint potentials (mV vs. NHE) for appearance and disappearance of W(V) species in *P. furiosus* AOR and *T. litoralis* FOR, and EPR parameters of related tungsten enzymes and model complexes

Sample/species	g_{av}	A_{av}	g_1	g_2	g_3	A_1	A_2	A_3	E_m (pH 8) W(V)		Ref.
									Appearance	Disappearance	
As-isolated Pf AOR and Tl FOR											
Pf AOR low-potential[a]	1.918	42	1.989	1.901	1.863	52	27	46	−436	−365	[39]
Tl FOR low-potential[a]	1.906	45	1.977	1.898	1.843	57	28	~50[b]	−335	−280	This work
Pf AOR mid-potential	1.963	–	1.988	1.961	1.940	–	–	–	−345	> +100	[39]
Tl FOR mid-potential	1.957	–	1.983	1.956	1.932	–	–	–	−34	> +175	This work
Pf AOR high-potential[a]	1.949	51	1.992	1.962	1.892	48	43	62	+157	> +300	[39]
Tl FOR high-potential[a]	1.940	48	1.981	1.956	1.883	45	40	59	+184	> +350	This work
Sulfide-activated Tl FOR											
Tl FOR mid-potential	1.954	–	1.981	1.950	1.931	–	–	–	−265	> 0	This work
Tl FOR high-potential	1.942	–	1.981	1.952	1.895	–	–	–	+65	> +275	This work
W-substituted rat liver sulfite oxidase											
low-pH W(V) (high Cl^-)	1.91	~54	1.98	1.89	1.87	81	~41	~41	–	–	[51]
high-pH W(V)	1.88	–	1.93	1.87	1.84	–	–	–	–	–	[51]
Models											
cis,trans-WO(SPh)L[c]	1.90	60	2.006	1.864	1.855	84	41	53	–	–	[55]
cis,trans-WO(SH)L	1.90	–	1.999	1.857	1.844	86	~40	–	–	–	[55]
$[WO(SPh)_4]^-$	1.936	55.1	2.018	1.903	1.903	78	44	44			[58]
$[WO(bdt)_2]^-$ [d]	1.962	52	2.044	1.931	1.911	78	40	37	–	–	[59]

[a] *g*-values (±0.001) and *A*-values ($\pm 2 \times 10^{-4}$ cm^{-1}) determined by simulation of natural abundance and ^{183}W-enriched spectra
[b] The larger linewidth at g_3 precludes the precise determination of the A_3 value for this resonance
[c] L = *N,N*-dimethyl-*N,N*-bis(mercaptophenyl)ethylenediamine
[d] bdt = 1,2-benzenedithiolate

signal accounts for 25–35 % of the total W in the enzyme.

The mid-potential and high-potential W(V) species are observed at higher potentials when the low-potential W(V) signal is no longer observable. These resonances are similar to the mid-potential and high-potential species observed in redox titrations of Pf and ES-4 AOR, albeit with *g*-values slightly lower than the equivalent AOR species (see Table 1). The mid-potential species in Tl FOR [$g = 1.983, 1.956, 1.932$ (Fig. 4b)] appears with a midpoint potential of -34 ± 20 mV and persists up to at least +175 mV (Fig. 3). Surprisingly, the midpoint potential of the mid-potential species in Tl FOR is more than 300 mV higher than the equivalent species in Pf AOR: $E_m = -34$ mV in Tl FOR versus −345 mV in Pf AOR. Above +175 mV the mid-potential species is difficult to see as it is obscured by the more intense high-potential species ($g = 1.981$, 1.956, 1.883 (Fig. 4c), which appears with a midpoint potential of $+184 \pm 20$ mV (compared to +157 mV in Pf AOR) and persists up to the highest potential obtained, +350 mV. As for the low-potential signal, the high-potential signal was simulated (Fig. 4c), in order to determine the anisotropic *g* and $A(^{183}W)$ parameters listed in Table 1. Spin quantitations indicate that the mid-potential species is a minor species accounting for less than 0.05 spins/W, whereas the high-potential species accounts for 0.35 spins/W. Both the mid- and high-potential W(V) species were also observed in samples of as-isolated Tl FOR that were exposed to O_2 for 25 min at room temperature. Moreover, reductive titrations have established that the redox processes involving the $[Fe_4S_4]^{2+,+}$ cluster and the low-, mid-, and high-potential W(V) species are fully reversible over the potential range −525 mV to +380 mV.

VTMCD studies of Tl FOR

Having established the conditions required to generate the optimal concentration of low-potential and high-potential W(V) species in Tl FOR, VTMCD spectroscopy was then used in an attempt to assess their excited state properties. In contrast to Pf AOR, in which the low-potential species is completely converted to the diol-inhibited form upon addition of glycerol or ethylene glycol, Tl FOR provided an opportunity to investigate the VTMCD properties of this functional species that is common to both FOR and AOR. Since the low-potential species could not be generated by incubation with substrate, as in Pf AOR, samples of Tl FOR were poised at potentials in the range of −350 to −280 mV in the presence of 55 % glycerol or poly(ethylene glycol) (PEG). Although significant concentrations of the low-potential W(V) species (about 0.1 spins/W) were obtained by the procedure, as evidenced by parallel EPR studies, no significant VTMCD signal, over and above that of the $[Fe_4S_4]^+$ cluster, was apparent. We conclude that the low-potential W(V) species has very weak VTMCD intensity.

The VTMCD spectra of the high-potential W(V) species was obtained by adding 55 % (v/v) glycerol to

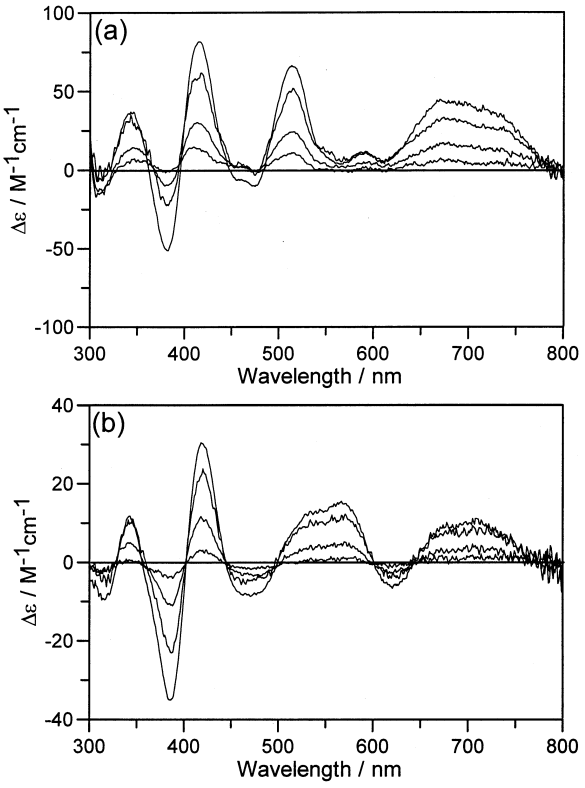

Fig. 5 **a** VTMCD spectra of the high-potential W(V) species in Tl FOR. The high-potential W(V) species (spin concentration = 0.3 spins/W) was prepared by adding 55 % (v/v) glycerol to a sample and exposing it to air for 45 min. The final sample concentration was 0.12 mM in FOR and the spectra were recorded at temperatures of 1.70, 4.22, 10.1, and 24.2 K with a magnetic field of 4.5 T. The intensity of all transitions increases with decreasing temperature. **b** VTMCD spectra of the sulfide-activated mid-potential W(V) species in Tl FOR. The sample was prepared by adding 55 % (v/v) glycerol to sulfide-activated Tl FOR that had been exposed to air for 45 min, followed by treatment with a 100-fold stoichiometric excess of KCN. The resulting sample (0.13 mM in FOR) exhibited only the sulfide-activated mid-potential W(V) EPR signal (spin concentration = 0.1 spins/W). MCD spectra were recorded at temperatures of 1.70, 4.22, 9.92, and 24.0 K with a magnetic field of 6.0 T

Tl FOR that was oxidized by exposure to air for 25 min (Fig. 5a). Concurrent EPR studies showed the high-potential W(V) resonance to be unchanged by the presence of the glycerol and spin quantitation indicated that the resonance accounted for about 0.35 spins/W. The VTMCD spectra consists of a broad positive band centered at about 670 nm, along with three sharp positive bands at 345, 410, and 510 nm and two negative bands at 380 and 460 nm. Near-IR VTMCD studies show an additional negative band at 880 nm, and MCD magnetization studies confirm an $S = 1/2$ ground state for all the observed transitions. This spectrum is very similar to that of the high-potential species in Pf AOR [39], confirming that the same W(V) high-potential species is present in both enzymes.

Sulfide activation and cyanide inactivation of Tl FOR

Sulfide activation

As-purified samples of Tl FOR (10 mg/mL) in 100 mM Tris/HCl (pH 8.0) buffer, and exhibiting a specific activity of 6.0 units/mg, were incubated with excess sodium sulfide (20 mM) and sodium dithionite (20 mM) under anaerobic conditions, both taken from stock solutions made up in 100 mM Tris/HCl buffer, pH 8. This lead to an approximately 8-fold enhancement in specific activity over a period of 10 h (Fig. 6a) and no further enhancement of activity was observed for longer incubation periods. No significant activation was observed with either sulfide or dithionite alone. DTT was ineffective as the reductant in place of dithionite in the activation mechanism. Clearly, both sulfide and dithionite are required for the activation process.

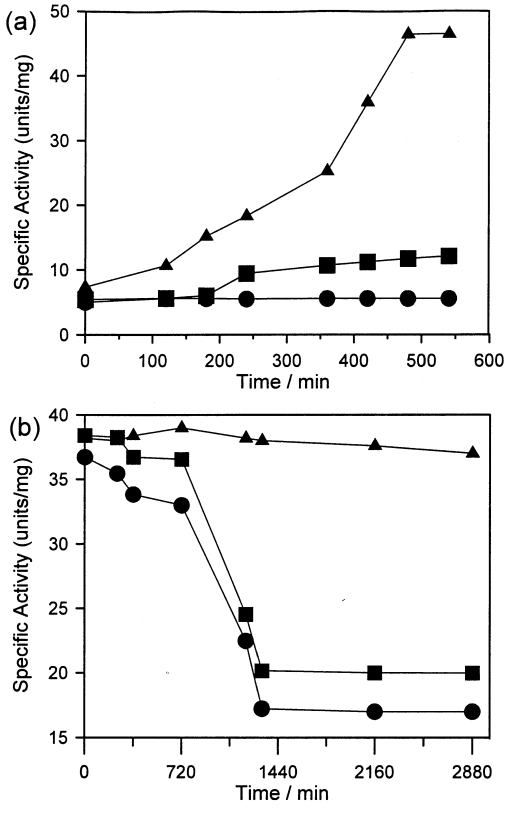

Fig. 6 **a** Activation of as-isolated Tl FOR by sulfide. The enzyme (10 mg/mL) in 100 mM Tris/HCl buffer, pH 8, was incubated at 23 °C with either 20 mM sodium sulfide (■), 20 mM sodium dithionite (●), or both (▲). At the indicated times, samples were removed and the residual activities were determined using formaldehyde as the substrate under standard assay conditions. **b** Cyanide inactivation of sulfide-activated Tl FOR. After removal of excess sulfide and dithionite, the enzyme (13 mg/mL) in 100 mM Tris/HCl buffer was incubated at 23 °C with 2 mM thionin and 5 mM cyanide (●) or 5 mM cyanide alone (■). The control to which neither thionin or cyanide was added is shown by the filled triangles (▲)

An oxidative redox titration monitored by EPR spectroscopy was performed on sulfide-activated Tl FOR (specific activity of 45 units/mg) in order to monitor changes in the $[Fe_4S_4]$ cluster or the W center. EPR studies at 4.2 K revealed that the redox and spectroscopic properties of the $[Fe_4S_4]$ cluster were unchanged on sulfide activation. There were, however, significant differences in the W(V) species observed in redox titrations using sulfide-activated samples compared to those of the as-isolated enzyme (compare Figs. S3 and S4 in the Supplementary material). The *g*-values and redox properties of the W(V) species observed during an oxidative redox titration of sulfide-activated Tl FOR are listed in Table 1 and spectra of samples poised at −148 mV and +197 mV are shown in Fig. 7a and b, respectively.

Immediately noticeable upon increasing the potential of the sulfide-activated sample was the absence of the low-potential signal. Indeed, no resonances attributable to a W(V) species were observed in the potential range where the low-potential W(V) species are seen in as-isolated Tl FOR and Pf AOR. The first resonance assignable as a W(V) species, the sulfide-activated mid-potential species, $g = 1.981$, 1.950, and 1.931, starts to appear at potentials > -300 mV, reaches maximum intensity at approximately −148 mV (Fig. 7a), and persists up to at least 0 mV. At potentials above +50 mV, a complex pattern of W(V) resonances develops (Fig. 7b). There are a total of three distinct W(V) species present at these higher potentials. All three species have very similar g_1 and g_2 values (g_1 in the range of 1.980–1.983 and g_2 in the range1.950–1.956), but are identifiable by their differing values of g_3. Our current understanding and assignment of the *g*-values for these resonances is as follows. One resonance corresponds to the sulfide-activated mid-potential species ($g = 1.981$, 1.950, and 1.931). One signal corresponds to a minor amount of

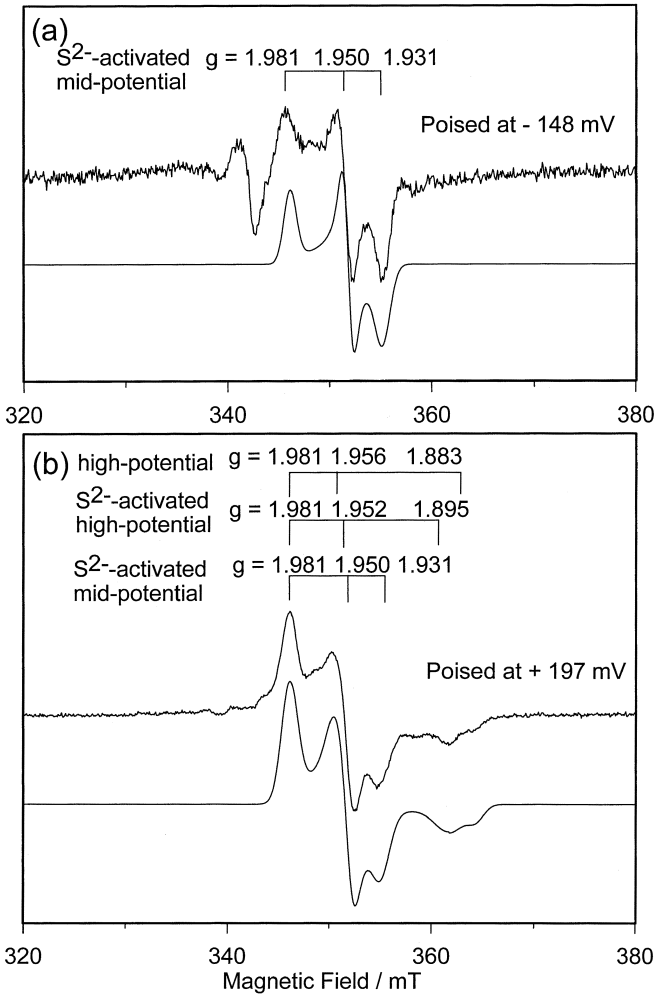

Fig. 7 X-band EPR spectrum and simulation of the sulfide-activated Tl FOR sample poised at −148 mV (**a**) and +197 mV (**b**) during ferricyanide oxidation in the presence of redox dyes. **a** The sulfide-activated mid-potential W(V) species in the sample poised at −148 mV and was simulated using $g_{1,2,3} = 1.981$, 1.950, 1.931 and $l_{1,2,3} = 0.69$, 0.59 and 0.84 mT. **b** The complex resonance in the sample poised at +197 mV has been simulated as the sum of sulfide-activated high-potential, mid-potential, and as-isolated high-potential spectra. Each was simulated separately and summed together in the ratio of 50:45:5, respectively, to obtain the final spectrum. The simulation parameters used were: sulfide-activated high-potential, $g_{1,2,3} = 1.981$, 1.952, 1.895; $l_{1,2,3} = 0.69$, 0.59, and 3.41 mT; sulfide-activated mid-potential, $g_{1,2,3} = 1.981$, 1.950, 1.931; $l_{1,2,3} = 0.69$, 0.59, and 0.84 mT; high-potential, $g_{1,2,3} = 1.981$, 1.956, 1.883; $l_{1,2,3} = 0.65$, 0.59, and 1.04 mT; where *l* is the linewidth. EPR conditions: temperature, 40 K; microwave power, 1 mW; modulation amplitude, 0.643 mT; microwave frequency, 9.60 GHz

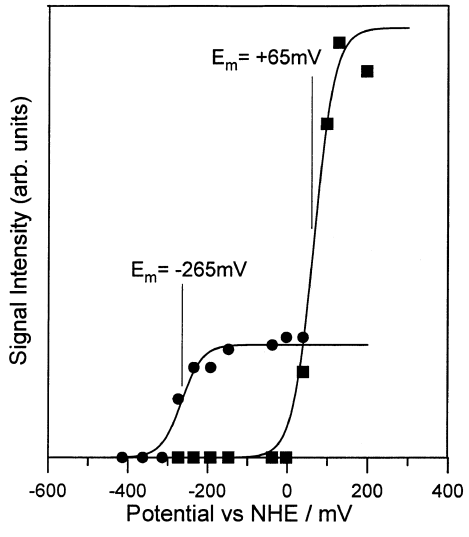

Fig. 8 EPR signal intensities (arbitrary units) for sulfide-activated Tl FOR (0.125 mM) as a function of poised potential. Dye-mediated redox titrations were carried out as described in Materials and methods. Intensity of the $g = 1.932$ feature of the sulfide-activated mid-potential W(V) species (●) and intensity of the $g = 1.897$ feature of the sulfide-activated high-potential W(V) species (■) were measured at 40 K. The *solid lines* are best fits to one-electron Nernst equations. The midpoint potentials used in constructing the Nernst plots are indicated on the figure. EPR conditions: temperature, 40 K; microwave power, 2 mW; modulation amplitude, 1.02 mT; microwave frequency, 9.60 GHz

the high-potential species previously observed in the enzyme as-isolated (there is a small peak at $g = 1.883$, which represents the g_3 of the high-potential signal). The third resonance has $g = 1.981$, 1.952, and 1.895 and corresponds to a sulfide-activated high-potential species. Plots of the intensity of the g_3 peaks of the sulfide-activated mid- and high-potential W(V) signals with respect to sample potential are shown in Fig. 8. Each was fit to a single one-electron Nernst plot to obtain mid-point potentials of -265 ± 20 mV for the appearance of the sulfide-activated mid-potential W(V) species and $+65 \pm 20$ mV for the appearance of the sulfide-activated high-potential W(V) species. Hence, although the *g*-values of the mid-potential sulfide-activated Tl FOR are unperturbed compared to the as-isolated enzyme, the mid-point potential decreases by about 230 mV (Table 1). A limited set of data points was also obtained under reductive conditions to check the reversibility of the redox titration. All three species were lost on reduction at approximately the same potential as they appeared during the oxidative titration and no new signals were observed.

In order to quantify the individual components present in the sulfide-activated redox titration, the EPR resonances of each of three species were simulated separately by matching the intensity of the g_3 peak with that observed in the redox titration sample poised at +197 mV. These simulations were then summed to obtain the complete spectrum (Fig. 7b). The data suggest that the sulfide-activated high- and mid-potential W(V) species are present in almost equal amounts and the three resonances occur in approximately the ratios of 50:45:5 for the sulfide-activated high-potential, sulfide-activated mid-potential, and high-potential W(V) species, respectively. However, spin quantitation of the sample poised at +197 mV indicates that all three W(V) resonances together account for only a total of 0.15 ± 0.05 spins/W. This compares to a total of 0.40 spins/W for as-isolated Tl FOR at the same potential, with the high-potential W(V) species accounting for 0.35 spins/W and the mid-potential W(V) species accounting for 0.05 spins/W.

Cyanide inactivation

The activity of as-isolated Tl FOR was unaffected by incubation with a 40-fold excess of potassium cyanide for a period of 4 days. However, sulfide-activated samples showed a pronounced cyanide inactivation (Fig. 6b). After chromatographic removal of excess sulfide, the activity of sulfide-activated Tl FOR decreased by about 20 %. The resultant sulfide-activated sample that was used for cyanide inactivation experiments had a specific activity of 37 units/mg and the activity remained essentially unchanged for upon incubation at room temperature for 24 h (Fig. 6b). Two different cyanide inactivation procedures were then followed: (1) the sample was oxidized with 2 mM thionin followed by the addition of 40-fold excess cyanide (5 mM), and then incubated for 24 h under anaerobic conditions; (2) the sample was directly treated with a 40-fold excess of cyanide (5 mM) for 48 h. In both cases there is an approximately 60 % loss of specific activity (Fig. 6b) after a period of 22 h. However, no further loss of activity was observed for the next 4 days under anaerobic conditions. Surprisingly, the residual activity of the cyanide-inactivated Tl FOR sample (15 units/mg) is still three-fold higher than the activity of the as-isolated enzyme. Similar sulfide activation and cyanide inactivation has been observed in Pf FOR [38].

The effect of cyanide on the spectroscopic properties of the tungsten center in Tl FOR was investigated by EPR spectroscopy. Sulfide-activated Tl FOR samples, poised at different potentials, were investigated by EPR before and after incubation with excess cyanide. The enzyme sample poised at -38 mV, which exhibited the sulfide-activated mid-potential EPR signal, was incubated with a 100-fold excess of potassium cyanide at room temperature under anaerobic conditions for 10 min. The EPR spectrum of the sample showed no significant changes (data not shown). Further incubation with cyanide for up to 3 h and even heating the sample to 80 °C for 15 min did not alter the signal. Hence cyanide appears to have no effect on the species responsible for the sulfide-activated mid-potential EPR spectrum.

A similar procedure was followed to probe the effects of cyanide on the sulfide-activated Tl FOR sample poised at +197 mV and exhibiting a mixture of sulfide-activated high- and mid- potential EPR signals (along with a minor component of the as-isolated high-potential signal) (Fig. 9a). Addition of a excess of potassium cyanide to the EPR sample and incubation for 10 min at room temperature under anaerobic conditions resulted in the disappearance of the sulfide-activated high-potential and as-isolated high-potential signals. The resulting EPR spectrum showed only the sulfide-activated mid-potential signal (Fig. 9b). Additional incubation of the sample for 30 min at room temperature and even heating to 60 °C for 15 min did not change the EPR spectrum any further. Subtraction of the spectrum obtained after cyanide treatment from the initial spectrum results in a spectrum almost identical to that of the sulfide-activated high-potential signal (Fig. 9c). Hence the sulfide-activated high-potential W(V) species is lost on incubation with cyanide.

In order to investigate the effects of oxygen on sulfide-activated Tl FOR, a sample poised at -7 mV (Fig. 10a), which showed only the sulfide-activated mid-potential W(V) signal, was exposed to air for varying amounts of time. After 15 min of exposure to air, there is a six-fold increase in the signal intensity due to the emergence of intense as-isolated and sulfide-activated high-potential signals at $g = 1.981$, 1.956, 1.883

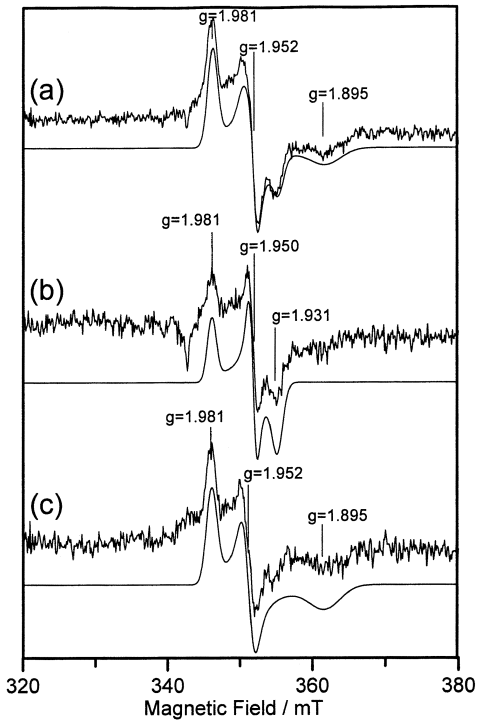

Fig. 9a–c Effect of anaerobic treatment of KCN solution on the sulfide-activated high-potential species of Tl FOR. **a** EPR spectrum of sulfide-activated W(V) species poised at +197 mV by ferricyanide oxidation in the presence of redox dyes. **b** EPR spectrum of sample **a** after addition of a 100-fold stoichiometric excess KCN solution. **c** Resultant spectrum after subtraction of spectrum **b** from spectrum **a**. The *lower traces* are the simulations of the $I = 0$ component of spectra **a**, **b**, and **c** as the sum of the sulfide-activated mid- and high-potential species, sulfide-activated mid-potential species, and sulfide-activated high-potential species, respectively. [Spectra **a** and **c** also appear to contain a minor component (5–10 %) of the as-isolated high-potential species which has been omitted from the simulations for clarity.] The simulation parameters are as listed in Fig. 7b and the EPR conditions are the same as described in Fig. 7

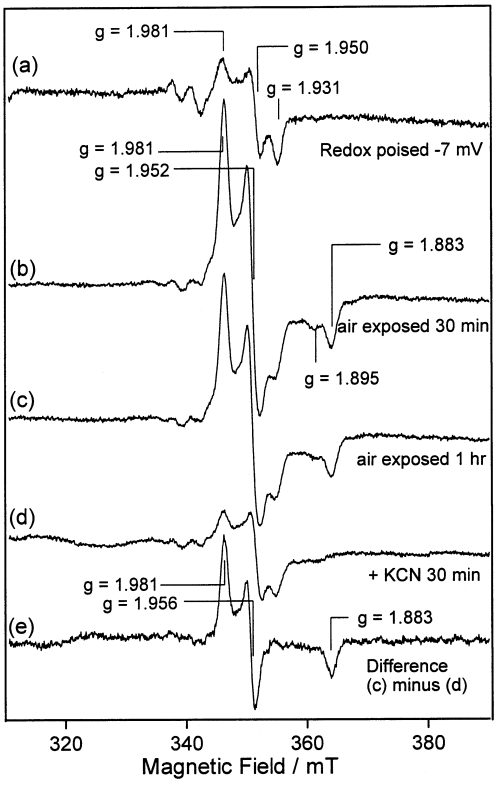

Fig. 10a–e Effect of air oxidation on the sulfide-activated mid-potential species of Tl FOR. **a** EPR spectrum of sulfide-activated W(V) species poised at −7 mV by ferricyanide oxidation in the presence of redox dyes. **b** EPR spectrum of sample **a** after exposing to air for 15 min. **c** EPR spectrum of sample **a** after exposing to air for 1 h. **d** EPR spectrum of sample **c** after addition of excess KCN solution. **e** Resultant spectrum after subtraction of spectrum **d** from spectrum **c**. The EPR conditions are the same as described in Fig. 7

and $g = 1.981$, 1.952, 1.895, respectively (Fig. 10b). Further exposure of the sample to air for 1 h resulted in additional conversion of the sulfide-activated high-potential species into as-isolated high-potential species (Fig. 10c). This O_2-induced conversion of the sulfide-activated high-potential species into the as-isolated high- potential species was confirmed by exposing samples containing optimal amounts of the sulfide-activated high-potential species to air at room temperature and re-recording the EPR spectrum (data not shown). Aerobic addition of a 100-fold excess of potassium cyanide to the sample shown in Fig. 10c and incubation for 10 min resulted in the disappearance of the high-potential signal, $g = 1.981$, 1.956, 1.883, leaving the mid-potential species (Fig. 10d). Moreover, subtraction of the spectrum after cyanide treatment (Fig. 10d) from the spectrum prior to cyanide treatment (Fig. 10c) reveals the as-isolated high-potential EPR signal in isolation (Fig. 10e). Hence, we conclude that oxygen converts the sulfide-activated high-potential species into the as-isolated high-potential species and that both types of high-potential signal are lost upon incubation with cyanide.

The ability to obtain homogeneous sulfide-activated mid-potential species via cyanide treatment affords the opportunity to obtain VTMCD spectra of this W(V) species (Fig. 5b). The MCD spectra comprise five positive *C*-terms at 700, 565, 535, 420, and 344 nm and three negative *C*-terms at 626, 475, and 382 nm. Comparison of the VTMCD spectrum of the as-isolated high-potential and sulfide-activated mid-potential species shown in Fig. 5a and b, respectively, shows differences in the low-energy charge-transfer bands above 550 nm. However the close similarity in the higher energy regions of the VTMCD spectrum, as well as in the g_1 and g_2 values, suggests that these are related species in terms of their ground and excited state properties.

Discussion

The EPR and VTMCD studies of Tl FOR presented herein, coupled with the previous studies of Pf AOR [39], facilitate a detailed comparison of the electronic and redox properties of the W and Fe-S centers at the active site of two W-containing ferredoxin oxidoreductases with different substrate specificities. In addition, these spectroscopic studies of Tl FOR provide the first direct assessment of the changes in active site properties that accompany sulfide activation in this class of enzyme. Since these enzymes are found in organisms that grow in strongly sulfiding environments in nature [5], sulfide-activated forms are likely to correspond more closely to the physiologically relevant species.

The gene sequence and subunit size of Pf AOR and Tl FOR are similar with ~60 % similarity and ~40 % identity, and all the residues involved in interactions with the bis-pterin-cofactor W center and nearby $[Fe_4S_4]$ cluster are conserved [8, 35]. However, Pf AOR is a dimer with two EXXH motifs that coordinate a mononuclear Fe center at the subunit interface, whereas this motif is absent in the tetrameric Tl FOR. In the case of *Pyrococcus* ES-4 AOR, a mononuclear Fe^{2+} center was evident by a $g = 16$ resonance in the parallel and perpendicular mode EPR spectra. The absence of this resonance and the EXXH motif in Tl FOR argues against a subunit bridging Fe center in Tl FOR. Moreover, Tl FOR is virtually identical to Pf FOR, 92 % similarity and 87 % identity [38], and the recent crystal structure of this enzyme confirms the tetrameric quaternary structure with no subunit bridging Fe center [19]. Hence, in addition to the $[Fe_4S_4]$, W, and Mg metal sites, that are common to all W-containing ferredoxin aldehyde oxidoreductases, Tl FOR is likely to contain the mononuclear Ca center that was found in each subunit of Pf FOR [19, 38].

$[Fe_4S_4]^{2+,+}$ cluster

The ground and excited state electronic properties of the $[Fe_4S_4]^+$ cluster in Tl FOR have been investigated by the combination of EPR and VTMCD spectroscopies. This work and previous studies of AORs and FORs indicate that these two types of W enzymes are readily distinguished by the EPR properties of their $[Fe_4S_4]^+$ clusters [5, 25, 39]. Both have predominantly $S = 3/2$ ground states and similar midpoint potentials ($E_m = -350$ mV and -368 mV for Pf AOR and Tl FOR, respectively), but exhibit quite distinct EPR signals due to different rhombicities ($E/D = 0.12$ and 0.33 for AOR and FOR, respectively). In the case of Tl FOR the cluster exists as a pH- and medium-dependent mixture of $S = 3/2$ and $S = 1/2$ ($g = 2.03$, 1.93, 1.86) ground states, whereas in Pf AOR the ground state properties are invariant with pH (over the range pH 6–10) and are not affected by addition of up to at least 70 % (v/v) glycerol or ethylene glycol. The structural origin of the different ground state properties of the clusters in AOR and FOR are not apparent from the crystal structures of Pf FOR and AOR [8, 19]. Both are coordinated by the same arrangement of four Cys residues and all the major hydrogen-bonding interactions are preserved. This underscores the exquisite sensitivity of the ground state properties of $[Fe_4S_4]^+$ clusters to changes in the cluster environment and the difficulty of correlating changes in ground state properties with differences in cluster structure or environment.

Tungsten center

EPR and VTMCD studies of Pf AOR revealed heterogeneity in the W center, with seven distinct W(V) species observed during dye-mediate titrations. In contrast, only three W(V) species were observed during redox titrations of as-isolated Tl FOR, corresponding to the low-potential, mid-potential, and high-potential W(V) species of Pf AOR. Inactive samples of Pf AOR exhibit a complex EPR signal spanning 600 mT that results from weak spin coupling between a W(V) species [E_m(W(VI)/W(V)) = -450 mV] and the $S = 3/2$ $[Fe_4S_4]^+$ cluster [39, 50], and this spin-coupled W(V) species exhibits a VTMCD spectrum comparable in intensity to that of the $S = 3/2$ $[Fe_4S_4]^+$ cluster. Conversion to this inactive form progressively occurs during prolonged anaerobic purification of Pf AOR in the presence of dithionite and the inactivation process has been tentatively attributed to reductive loss of one of the dithiolene ligands to give a dioxo-W(VI) species that is only reducible to the monooxo-W(V) state over the physiological potential range [5, 39]. EPR alone is not necessarily a reliable criterion for detecting a similar spin-coupled W(V) species in Tl FOR. The breadth of the resonance resulting from weak spin-coupling is critically dependent on the magnitude of the coupling and the intrinsic linewidths of the resonances from the "uncoupled" paramagnets. Since the rhombic $S = 3/2$ $[Fe_4S_4]^+$ resonance in Tl FOR has much greater linewidths that the more axial $S = 3/2$ $[Fe_4S_4]^+$ resonance in Pf FOR, detection of a spin-coupled resonance would be expected to be more difficult in Tl FOR. However, weak spin-coupling does not significantly perturb the VTMCD of the paramagnetic chromophores. Consequently, the observation that the VTMCD spectrum and magnetization data of dithionite-reduced Tl FOR corresponds to that of $S = 3/2$ $[Fe_4S_4]^+$, with no evidence for a W(V) species, demonstrates that all of the W is diamagnetic, i.e. W(VI) or W(IV), in the enzyme as-isolated. While this result does not rule out the presence of a dioxo-W(VI) species in Tl FOR equivalent to that proposed in inactive preparations of Pf AOR, it demonstrates that such a species, if present, must have a W(VI)/W(V) midpoint potential < -450 mV.

A low-potential magnetically isolated W(V) species, $g = 1.97–1.99, 1.90, 1.84–1.86$, is shown to be common to both AORs and FORs [39]. This resonance increases and subsequently decreases in intensity in oxidative redox titrations, indicative of closely spaced W(IV)/W(V) and W(V)/W(VI) couples, and is maximal at −400 mV in Pf AOR, −350 in ES-4 AOR, and −310 mV in Tl FOR. Maximally it accounts for approximately 0.15–0.20 spins/W, which translates to a W species corresponding to approximately 30 % of the W in each enzyme, given the close separation of the midpoint potentials. However, the low-potential W(V) species in Tl FOR differs in three important respects from those found in AORs. First, it cannot be generated by incubation with formaldehyde at 80 °C, possibly due to the 80–100 mV higher midpoint potentials for the W(IV)/W(V) and W(V)/W(VI) couples in Tl FOR. Second, it is not converted into the diol-inhibited W(V) species by anaerobic treatment with high concentrations (55 % v/v) of diols such as glycerol or ethylene glycol at 85 °C. This is in accord with suggestion that this pool of W is catalytically competent, since in contrast to Tl FOR, AORs are known to be inhibited by high concentrations of diols [5, 39]. Third, it is lost together with a 6- to 8-fold enhancement of enzymatic activity in sulfide-activated samples of Tl FOR. In contrast, an equivalent "sulfide-activation" procedure did not alter the activity or EPR/redox properties of the W center in Pf AOR (data not shown). By analogy with xanthine oxidase [4], this type of behavior suggests that the low-potential W(V) species corresponds to a desulfo form of the enzyme. In AORs, this desulfo form of the enzyme appears to be responsible for the observed catalytic activity, and accordingly the activity is not inhibited by cyanide. In contrast, catalytic activity in Tl FOR is primarily or exclusively associated with the sulfide-activated form that is subject to cyanide inhibition. As yet it has not been possible to identify a W(V) species associated with the functional sulfide-activated form of Tl FOR at potentials down to −450 mV. EPR and VTMCD studies of sulfide-activated forms of Tl FOR using low-potential reductants, i.e. Ti(III) citrate and deazaflavin mediated photochemical reduction, are planned to address this question.

Our current working model for the structure of the low-potential W(V) species in AORs and FORs is shown in Fig. 11. In large part this model is based on the close similarity in the *g*-values and ^{183}W *A*-values with those of the low-pH W(V) species in W-substituted sulfite oxidase [51] (Table 1) and the available crystallographic data for Pf AOR and FOR [8, 19].

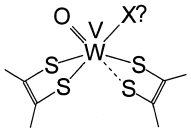

Fig. 11 Proposed model for low-potential W(V) species. The nature of hypothetical ligand X is discussed in the text

The EPR studies of the low-pH W(V) species in W-substituted sulfite oxidase indicate a W coordination environment identical to that of the equivalent low-pH Mo(V) species, i.e. one oxo, one hydoxide, one cysteinyl sulfur, two sulfurs from a single pterin-cofactor dithiolene, and one chloride (only in high chloride samples) [52–54]. In general, EPR parameters of W(V) resonances exhibit a direct correlation between the g_{av} and A_{av} values and the number of thiolate ligands. The g_{av} increases and A_{av} decreases with the increasing thiolate coordination at the tungsten center [5]. The g_{av} values of structurally characterized four sulfur-coordinated oxo-thiolate W(V) complexes such as $[WO(SPh)_4]^-$ and $[WO(bdt)_2]^-$ are significantly higher than that of the low-potential form of the Tl FOR (Table 1). However, g_{av} of the recently published several three-sulfur-coordinated oxo-thiolate W(V) model complexes [55] of the type *cis,trans*-WO(X)L [$X = PhS^-$, SH^-; L = *N,N*-dimethyl-*N,N*-bis(mercaptophenyl)ethylenediamine] are in excellent agreement with those of the low-potential Tl FOR and low-pH form of the tungsten-substituted sulfite oxidase (Table 1). This raises the possibility that one of the dithiolene sulfur ligands is weakly coordinated to the tungsten center in the low-potential W(V) form. The nature of the proposed ligand X in the above model remains undetermined. Recent studies of the effect of H_2O/D_2O exchange on the low-potential EPR signal in Pf AOR did not show any significant change in linewidth, and hence provided no positive evidence for hydroxyl ligation (data not shown). However, EPR experiments involving the effects of different buffers and exogenous fluoride on the properties of the low-potential W(V) species in Pf AOR suggest that anions such as chloride or fluoride are able to bind at the W site (I.K. Dhawan, R. Roy, M.W.W. Adams and M.K. Johnson, unpublished results). Hence samples prepared in Tris/HCl buffers may have a weakly coordinated chloride at this site.

EPR redox titrations of both AORs and FORs reveal two additional W(V) species that appear at higher potentials. A minor "mid-potential" W(V) species, $g = 1.98–1.99$, 1.96, 1.93–1.94, accounting for < 0.05 spins/W, appears with midpoint potentials of −351 mV in Pf AOR and −34 mV in Tl FOR. At potentials above 0 mV, a major "high-potential" W(V) species, $g = 1.98–1.99$, 1.95–1.96, 1.88–1.89, accounting for 0.3–0.4 spins/W, appears with a midpoint potential of +157 mV in Pf AOR, +50 mV in ES-4 AOR, and +184 mV in Tl FOR, and persists up to at least +300 mV. Both W(V) resonances are the product of reversible redox processes in Tl FOR and both are perturbed in the sulfide-activated form of Tl FOR. Although the *g*-values and quantitation of the mid-potential species in the sulfide-activated sample are essentially unchanged, the midpoint potential decreases by ~230 mV. In the sulfide-activated sample, the high-potential EPR signal has a slightly higher g_3 value, a 120-mV lower midpoint potential, and an

intensity that is reduced at least three-fold. The high-potential and mid-potential W(V) species appear to be related species, but with some interesting and important differences. For example, both are formed in one-electron oxidation processes and persist up to highest potentials accessible in this study, both have similar g_1 and g_2 values, and both have similar VTMCD spectra below 550 nm, and have intense lower energy S-to-W(V) or W(V)-to-S charge transfer bands. However, in addition to markedly different midpoint potentials, the mid-potential and high-potential species differ significantly in their pattern of low-energy charge transfer bands in the VTMCD spectra and in their response to cyanide. The mid-potential species are not perturbed by cyanide, whereas the high-potential species are lost upon incubation with excess cyanide.

Although the high-potential W(V) species can account for as much as 30–40 % of the W in the enzyme, it does not appear to originate from a functional form of W. The main evidence for this is that it is observed without change in intensity or redox properties in samples that have been irreversibly inactivated by prolonged exposure to O_2. The observation that the high-potential species is observed with substantially reduced intensity in sulfide-activated Tl FOR also suggests that activation involves the inactive W centers that are responsible for producing the high-potential W(V) species. Moreover, it is formed at potentials that are unlikely to be physiologically relevant in light of the extremely low potentials of acid/aldehyde couples, < -500 mV, and it persists up to at least +300 mV. For these reasons, it is considered to be an artifact of ligand-based as opposed to W-based oxidation, although we currently have no direct experimental evidence in support of such a proposal. For the same reasons, the formation of the mid-potential species may also involve ligand-based oxidation of an active or inactive W center. The likelihood that the high-potential and mid-potential W(V) species are related is suggested by the similarity in EPR signals, which differ only in terms of the g_3 values. A particularly close relationship between the sulfide-activated high-potential and as-isolated high-potential W(V) species is evident from the observation that the former is converted into the latter by exposure to air and that both W(V) species disappear upon incubation with cyanide.

Although neither the as-isolated nor sulfide-activated forms of the mid-potential and high-potential W(V) species of Tl FOR are likely to be physiologically relevant in terms of the catalytic cycle, it is constructive to consider the nature of the species and the chemistry that could be responsible for the appearance of these resonances. We have considered two possible types of ligand-based oxidation that could correspond to net one-electron oxidations. One involves two-electron oxidation of one of the coordinated dithiolene ligands coupled with one-electron reduction of a

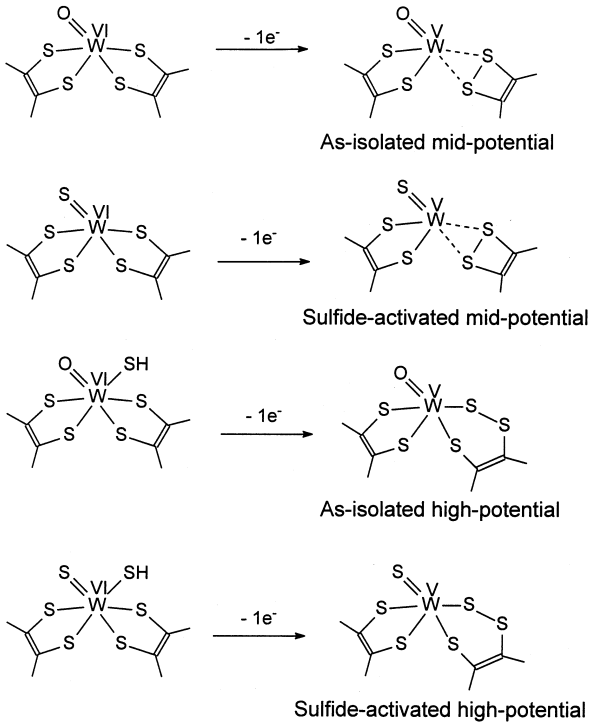

Fig. 12 Proposals for ligand-based redox chemistry and working models for the as-isolated and sulfide-activated forms of both the mid-potential and high-potential W(V) species

W(VI) center. In light of the inverse correlation between the Mo-S and dithiolene S-S distances for the enzyme structures in the protein database, a loosely attached disulfide ligand is considered to be the most likely product of the two-electron oxidation of the dithiolene ligand. The other requires a terminal S ligand (S^{2-} or SH^-), which would undergo two-electron oxidation and insertion into one of the W-S(dithiolene) bonds to form a W-trithiolene chelate ring, with concomitant one-electron reduction of the W(VI) center. Precedent for this type of reversible oxidative sulfur-insertion chemistry to form a trithiolenes comes from inorganic thio-Mo chemistry ([56] and references therein). In previous work, we argued that the high g_{av} values associated with the high-potential species favored structural models with four S ligands [39]. However, high g_{av} values could also result from the presence of low-energy charge transfer transitions, and it is not possible to discount either type of ligand-based redox chemistry at this stage.

Our current tentative working hypotheses for the nature and origin of the as-isolated and sulfide-activated forms of the mid-potential and high-potential W(V) species are summarized in Fig. 12. All are considered to arise from ligand-based, one-electron oxidation of W(VI) species with sulfide-activation entailing replacement of a terminal oxo ligand with a terminal sulfido ligand. The mid-potential species are proposed to be derived from dithiolene oxidation of monooxo- or monosulfido-W(VI) species, whereas the high-po-

tential species are proposed to be derived from oxidation and insertion of a terminal sulfido or thiol ligand (shown as a thiol in Fig. 12) to form a W-trithiolene chelate. The difference between the as-isolated and sulfide-activated forms of both the mid-potential and high-potential species is therefore tentatively attributed to the presence of a terminal oxo and sulfido ligand, respectively. The small changes in *g*-values between the as-isolated and sulfide-activated forms in both cases are consistent with EPR studies of Mo(V) complexes that differ only in terms of the terminal chalcogenide ligand, i.e. oxo or sulfido [57]. Both types of ligand-based oxidations might be expected to have low-energy charge transfer transitions, S-to-W(V) for the trithiolene or W(V)-to-S for the oxidized dithiolene, and loss of the high-potential EPR signals on addition of cyanide could result from a change in midpoint potential accompanying cyanide-binding or extraction of S^0 in the case of the trithiolene to form SCN^-. The latter is considered more likely since preliminary colorimetric experiments indicate the presence of SCN^- in cyanide-treated as-prepared and sulfide-activated samples. Although there is as yet no positive evidence for terminal sulfido or thiol ligation in any W-containing AOR, the approximately 8-fold increase in activity of Tl FOR on incubation with sulfide is interpreted in terms of replacement of a terminal oxo group by a terminal sulfido group in the W(VI) oxidation state, by analogy with xanthine oxidase [4]. Since tungsten-containing hyperthermophilic archaea, such as *Thermococcus litoralis*, thrive under sulfur-rich environments at elevated temperatures, physiological activity may well correspond to a species with partial or complete terminal sulfur ligation, as opposed to the crystallographically defined forms of Pf FOR [19] and Pf AOR [8], which appear to have exclusively an oxygenic terminal W ligand.

In light of the previous studies of Pf AOR which concluded that the as-isolated enzyme was heterogeneous with contributions from W(VI), W(V), and W(IV) species, one of the major goals of this study was to establish the conditions necessary for preparing homogeneous samples of Tl FOR, in order to elucidate the catalytic mechanism in this class of enzyme. Clearly the sulfide-activated form of Tl FOR is an important milestone in this endeavor, since the only observable W(V) species in redox titrations are the mid-potential and high-potential species which together account for only 15 % of the total W content and both are believed to originate from W(VI) species. Hence this form of the enzyme is likely to be exclusively in the W(VI) oxidation state as prepared in the presence of dithionite. Clearly there is a pressing need to investigate this form of the enzyme by crystallography, EXAFS, and resonance Raman in order to more precisely define the W coordination sphere, and to attempt reduction with lower potential reductants under more physiologically relevant conditions. Redox cycling between W(VI), W(V), and W(IV) states may not be possible at ambient temperatures, and even if this can be accomplished, it will be very difficult to investigate the catalytic mechanism by techniques such as EPR and VTMCD owing to spin coupling and/or spectral overlap of the paramagnetic W(V) and $[Fe_4S_4]^+$ species. While this study and the available crystallographic data suggest mechanistic parallels between this class of W-containing ferredoxin aldehyde oxidoreductases and the xanthine oxidase class of Mo-containing hydroxylases [19], establishing a detailed catalytic mechanism clearly presents a major challenge for modern biophysical techniques.

Acknowledgements This work was supported by grants from the National Science Foundation (MCB9808857 to M.K.J), the Department of Energy (FG09-88ER13901 to M.W.W.A.), and by a National Science Foundation Research Training Group Award to the Center for Metalloenzyme Studies (BIR-9413236). We thank Professor R. L. Belford for the EPR simulation program QPOW.

References

1. Young CG, Wedd AG (1994) In: King RB (ed) Encyclopedia of inorganic chemistry. Wiley, Chichester, pp 2330–2346
2. Pilato RS, Stiefel EI (1999) In: Reedijk J, Bouwman E (eds) Bioinorganic catalysis, 2nd edn. Dekker, New York, pp 81–152
3. Enemark JH, Young CG (1993) Adv Inorg Chem 40:1–88
4. Hille R (1996) Chem Rev 96:2757–2816
5. Johnson MK, Rees DC, Adams MWW (1996) Chem Rev 96:2817–2839
6. Rajagopalan KV (1991) Adv Enzymol Relat Areas Mol Biol 64:215–290
7. Rajagopalan KV, Johnson JL (1992) J Biol Chem 267:10199–10202
8. Chan MK, Mukund S, Kletzin A, Adams MWW, Rees DC (1995) Science 267:1463–1469
9. Kisker C, Schindelin H, Pacheco A, Garrett RM, Rajagopalan KV, Enemark JH, Rees DC (1997) Cell 91:973–983.
10. Romao MJ, Archer M, Moura I, Moura JJG, LeGall J, Engh R, Schneider M, Hof P, Huber R (1995) Science 270:1170–1176
11. Huber R, Hof P, Duarte RO, Moura JJG, Moura I, Liu MY, LeGall J, Hille R, Romao MJ (1996) Proc Natl Acad Sci USA 93:8846–8851
12. Schindelin H, Kisker C, Hilton J, Rajagopalan KV, Rees DC (1996) Science 272:1616–1622
13. Schneider F, Löwe J, Huber R, Schindelin H, Kisker C, Knablein J (1996) J Mol Biol 263:53–69
14. McAlpine AS, McEwan AG, Shaw AL, Bailey S (1997) JBIC 2:690–701
15. McAlpine AS, McEwan AG, Bailey S (1998) J Mol Biol 275:613–623
16. Czjzek M, Santos JD, Pommier J, Giordano G, Mejean V, Haser R (1998) J Mol Biol 284:435–447
17. Dias JM, Than ME, Humm A, Huber R, Bourenkov GP, Bartunik HD, Bursakoc S, Calvete J, Caldeira J, Carneiro C, Moura JJG, Moura I, Romao MJ (1999) Structure 6:65–79
18. Boyington JC, Gladyshev VN, Khangulov SV, Stadtman TC, Sun PD (1997) Science 275:1305–1308
19. Hu Y, Faham S, Roy R, Adams MWW, Rees DC (1999) J Mol Biol 286:899–914
20. Adams MWW, Kletzin A (1996) FEMS Microbiol Rev 18:5–63
21. Adams MWW (1994) In: King RB (ed) Encyclopedia of inorganic chemistry. Wiley, Chichester, pp 4284–4291

22. Mukund S, Adams MWW (1990) J Biol Chem 265:11508–11516
23. Mukund S, Adams MWW (1991) J Biol Chem 266:14208–14216
24. Heider J, Ma K, Adams MWW (1995) J Bacteriol 177:4757–4764
25. Mukund S, Adams MWW (1993) J Biol Chem 268:13592–13600
26. Mukund S, Adams MWW (1995) J Biol Chem 270:8389–8392
27. Yamamoto I, Saiki T, Liu S-M, Ljungdahl LG (1983) J Biol Chem 258:1826–1832
28. Deaton JC, Solomon EI, Watt GD, Wetherbee PJ, Durfor CN (1987) Biochem Biophys Res Commun 149:424–430
29. Huber C, Caldeira J, Jongejan JA, Simon H (1994) Arch Microbiol 162:303–309
30. White H, Simon H (1992) Arch Microbiol 158:81–84
31. Schmitz RA, Albracht SPJ, Thauer RK (1992) Eur J Biochem 209:1013–1018
32. Schmitz RA, Richter M, Linder D, Thauer RK (1992) Eur J Biochem 207:559–565
33. Schmitz RA, Albracht SPJ, Thauer RK (1992) FEBS Lett 309:78–81
34. Johnson JL, Rajagopalan KV, Mukund S, Adams MWW (1993) J Biol Chem 268:4848–4852
35. Kletzin A, Mukund S, Kelley-Crouse TL, Chan MK, Rees DC, Adams MWW (1995) J Bacteriol 177:4817–4819
36. Schindelin H, Kisker C, Rees DC (1997) JBIC 2:773–781
37. Mukund S (1995) PhD Dissertation. University of Georgia, Athens, Ga
38. Roy R, Mukund S, Schut GJ, Dunn DM, Weiss R, Adams MWW (1999) J Bacteriol 181:1171–1180
39. Koehler BP, Mukund S, Conover RC, Dhawan IK, Roy R, Adams MWW, Johnson MK (1996) J Am Chem Soc 118:12391–12405
40. George GN, Prince RC, Mukund S, Adams MWW (1992) J Am Chem Soc 114:3521–3523
41. Johnson MK (1988) In: Que L (ed) Metal clusters in proteins. (ACS symposium series, vol 372) American Chemical Society, Washington, pp 326–342
42. Thomson AJ, Cheeseman MR, George SJ (1993) Methods Enzymol 226:199–232
43. Belford RL, Nilges MJ (1979) In: Proceedings of the EPR Symposium at the 21st Rocky Mountain Conference, Denver, Colo
44. Nilges MJ (1979) PhD Dissertation. University of Illinois, Urbana, Ill
45. OnateYA, Finnegan MG, Hales BJ, Johnson MK (1993) Biochim Biophys Acta 1164:113–123
46. Lindahl PA, Day EP, Kent TA, Orme-Johnson WH, Münck E (1985) J Biol Chem 260:11160–11173
47. Johnson MK, Robinson AE, Thomson AJ (1982) In: Spiro TG (ed) Iron-sulfur proteins. Wiley-Interscience, New York, pp 367–406
48. Fu W, Drozdzewski PM, Davies MD, Sligar SG, Johnson MK (1992) J Biol Chem 267:15502–15510
49. Conover RC, Kowal AT, Fu W, Park J-B, Aono S, Adams MWW, Johnson MK (1990) J Biol Chem 265:8533–8541
50. Arendsen AF, de Vocht M, Bulsink YB, Hagen WR (1996) JBIC 1:292–296
51. Johnson JL, Rajagopalan KV (1976) J Biol Chem 251:5505–5511
52. Garrett RM, Rajagopalan KV (1996) J Biol Chem 271:7387–7391
53. George GN, Garrett RM, Prince RC, Rajagopalan KV (1996) J Am Chem Soc 118:8588–8592
54. George GN, Kipke CA, Prince RC, Sunde RA, Enemark JH, Cramer SP (1989) Biochemistry 28:5075–5080
55. Barnard KR, Gable RW, Wedd AG (1997) JBIC 2:623–633
56. Stiefel EI (1998) Pure Appl Chem 70:889–896
57. Young CG, Enemark JH, Collison D, Mabbs FE (1987) Inorg Chem 26:2925–2927
58. Hanson GR, Brunette AA, McDonnel AC, Murray KS, Wedd AG (1981) J Am Chem Soc 103:1953–1959
59. Oku H, Ueyama N, Nakamura A (1995) Chem Lett 621–622